Nanoscale

ROYAL SOCIETY OF CHEMISTRY

COMMUNICATION

View Article Online
View Journal | View Issue

Check for updates

Cite this: *Nanoscale*, 2024, **16**, 4563

Received 26th November 2023,
Accepted 16th January 2024

DOI: 10.1039/d3nr06015b

rsc.li/nanoscale

Published on 19 January 2024. Downloaded on 7/24/2025 8:30:23 AM.

A homologous series of macrocyclic Ni clusters: synthesis, structures, and catalytic properties†

Huixin Xiang,‡[a,b] Ranran Cheng,‡[b] Chenhao Ruan,[a,b] Changqing Meng,[a,b] Yuzheng Gan,[a,b] Wanyu Cheng,[a] Yue Zhao,[c] Cong-Qiao Xu,*[d] Jun Li[d,e] and Chuanhao Yao*[a,b]

Due to their intriguing ring structures and promising applications, nickel–thiolate clusters, such as $[Ni_n(SR)_{2n}]$ (n = 4–6), have attracted tremendous interest. However, investigation of the synthesis, structures, and properties of macrocyclic Ni_n clusters (n > 8) has been seriously impeded. In this work, a homologous series of macrocyclic nickel clusters, $Ni_n(4MPT)_{2n}$ (n = 9–12), was fabricated by using 4-methylphenthiophenol (4MPT) as the ligand. The structures and compositions of the clusters were determined by single-crystal X-ray diffraction (SXRD) in combination with electrospray ionization mass spectrometry (ESI-MS). Experimental results and theoretical calculations show that the electronic structures of the clusters do not change significantly with the increase of Ni atoms. The coordination interactions between Ni and S atoms in $[NiS_4]$ subunits are proved to play a crucial rule in the remarkable stability of Ni clusters. Finally, these clusters display excellent catalytic activity towards the reduction of *p*-nitrophenol, and a linear correlation between catalytic activity and ring size was revealed. The study provides a facile approach to macrocyclic homoleptic nickel clusters, and contributes to an in-depth understanding of the structure–property correlations of nickel clusters at the atomic level.

[a]*Strait Institute of Flexible Electronics, Fujian Normal University, Fuzhou 350117, China. E-mail: ifechhyao@fjnu.edu.cn*
[b]*Institute of Flexible Electronics (IFE), Northwestern Polytechnical University, Xi'an 710072, China*
[c]*Coordination Chemistry Institute, State Key Laboratory of Coordination Chemistry, School of Chemistry and Chemical Engineering, Nanjing University, Nanjing 210023, China*
[d]*Department of Chemistry, Southern University of Science and Technology, Shenzhen 518055, China. E-mail: xucq@sustech.edu.cn*
[e]*Department of Chemistry and Engineering Research Center of Advanced Rare-Earth Materials of Ministry of Education, Tsinghua University, Beijing 10084, China*

†Electronic supplementary information (ESI) available. CCDC 2307845 (for $Ni_9(4MPT)_{18}$), 2307689 (for $Ni_{10}(4MPT)_{20}$), 2307690 (for $Ni_{11}(4MPT)_{22}$), and 2308123 (for $Ni_{12}(4MPT)_{24}$). For ESI and crystallographic data in CIF or other electronic format see DOI: https://doi.org/10.1039/d3nr06015b

‡These authors contributed equally to this work.

Chuanhao Yao

Chuanhao Yao received his Ph.D. degree from the University of Chinese Academy of Sciences in 2016. Subsequently, he carried out postdoctoral research at the Department of Chemistry, National University of Singapore (NUS). He attained his professor position at Northwestern Polytechnical University (NPU) in 2019, and in early 2023, he moved to Fujian Normal University as a full professor. His research interests are focused on the design, synthesis and characterization of atomically precise metal clusters and their applications in catalysis, biomedicine, and light-emitting and flexible electronic devices.

1. Introduction

Metal clusters have attracted extensive interest due to their precise compositions as well as their well-defined structures, which provide excellent platforms to elucidate the relationships between their structures and properties.[1–5] The last two decades have witnessed breakthroughs in the synthesis, characterization, and property exploration of group 11 transition metal (Au, Ag, Cu) clusters and their alloys;[6–17] however, the study of the metal clusters composed of group 10 transition metals (Ni, Pd, Pt) is still limited. In particular, the synthesis of core–shell structured clusters is extremely challenging; instead, cyclic polynuclear, tiara-like Ni clusters are readily available.[18–31] The development of the cyclic polynuclear $Ni_6(SR)_{12}$ clusters dates back to the 1960s.[18,19] Since then, nickel clusters have received increasing attention, probably because of their low price and availability of large reserves of nickel compared to platinum and palladium.[21,25,28,32] As a medium-sized cyclic nickel cluster, Ni_6 clusters stabilized by

Published on 19 January 2024. Downloaded on 7/24/2025 8:30:23 AM.

diverse ligands have been intensively studied.[18–26,33,34] For example, Woodward and co-workers reported the first representative of a Ni_6 cluster, which was obtained from the reaction of diethyl disulfide with nickel carbonyl in benzene.[18] Subsequently, cyclic Ni_6 clusters stabilized by other thiol ligands have also been reported, and in-depth investigations into their structure and properties conducted.[19–26,33,34] In addition, smaller size nickel clusters such as Ni_4 and Ni_5 have also been prepared, and structure characterization results demonstrated that both have crown-like structures built up from approximately planar [NiS_4] units linked by bridged thiolate ligands.[27,29–32,35] Such series of small-ring Ni_n clusters (n = 4, 5, 6) are easy to prepare and display highly symmetric polygonal structures, probably because of their aromaticity.[27,36,37] The delocalization of the d-orbital electrons across the Ni_n rings leads to bond length equalization and thereby aromaticity.[27] The structures of the small Ni_n (n = 4, 5, 6) rings are not sensitive to the type of ligands utilized; however, this is not always the case when the size of clusters becomes larger. For example, ring-structured $Ni_8(SCH_2COOEt)_{16}$ was produced in 1985;[38] however, by using $NaSC_4H_9$ instead of the $HSCH_2COOEt$ ligand, a non-ring structured nickel sulfide thiolate cluster, [$Ni_8S(SC_4H_9)_9$], was reported by Henkel and coworkers.[39] In another contribution, the intriguing cyclic structures of $Ni_9(SPh)_{18}$ and $Ni_{11}(SPh)_{22}$ were determined by Dahl and coworkers, but $Ni_{10}(SPh)_{20}$ was not reported in their work.[40] Subsequently, the cyclic Ni_{10} and Ni_{12} were revealed, in which the nickel atoms were stabilized by two different types of thiolate ligands, but Ni_{11} was missing.[41] As a dodecanuclear cluster, $Ni_{12}(tBu_3SiS)_{12}Br_{12}$ was produced by Sydora and coworkers, and in this cluster, the nickel atoms are linked by a thiolate ligand and bromine atom to form a tetrahedral geometry, distinctly different from the planar [NiS_4] subunits previously reported.[42] These works make us wonder whether the homoleptic $Ni_9(SR)_{18}$, $Ni_{10}(SR)_{20}$, $Ni_{11}(SR)_{22}$, and $Ni_{12}(SR)_{24}$ do exist or not. Based on the discussion above, a consensus that ligands play an important role in dictating the structure of clusters, can be reached.[32,43–46] In other words, the structures of larger nickel clusters are sensitive to the ligands utilized. To date, the synthesis of larger sized nickel clusters is still challenging, and the in-depth structure–property understanding of the macrocyclic nickel clusters has been impeded.

Herein, we report the synthesis of a sequence of macrocyclic nickel clusters, $Ni_n(4MPT)_{2n}$ (n = 9–12), protected by the same ligand (4MPT = 4-methylphenthiophenol), where their compositions and structures are determined by electrospray ionization mass spectrometry (ESI-MS) in combination with single-crystal X-ray diffraction (SXRD). The results show that all these nickel clusters possess ring structures. The primary structures of $Ni_9(4MPT)_{18}$ and $Ni_{11}(4MPT)_{22}$ are similar to those of the reported $Ni_9(SPh)_{18}$ and $Ni_{11}(SPh)_{22}$.[40] However, the structures of the $Ni_{10}(4MPT)_{20}$, and $Ni_{12}(4MPT)_{24}$ are novel and distinct from the structures of Ni_{10} and Ni_{12} clusters protected by two kinds of thiolate ligands.[41] Most interestingly, although the clusters become larger with increased numbers of Ni atoms, their electronic structures and optical properties do not change dramatically. Finally, the reduction of *p*-nitrophenol catalyzed by these homologous series of nickel clusters

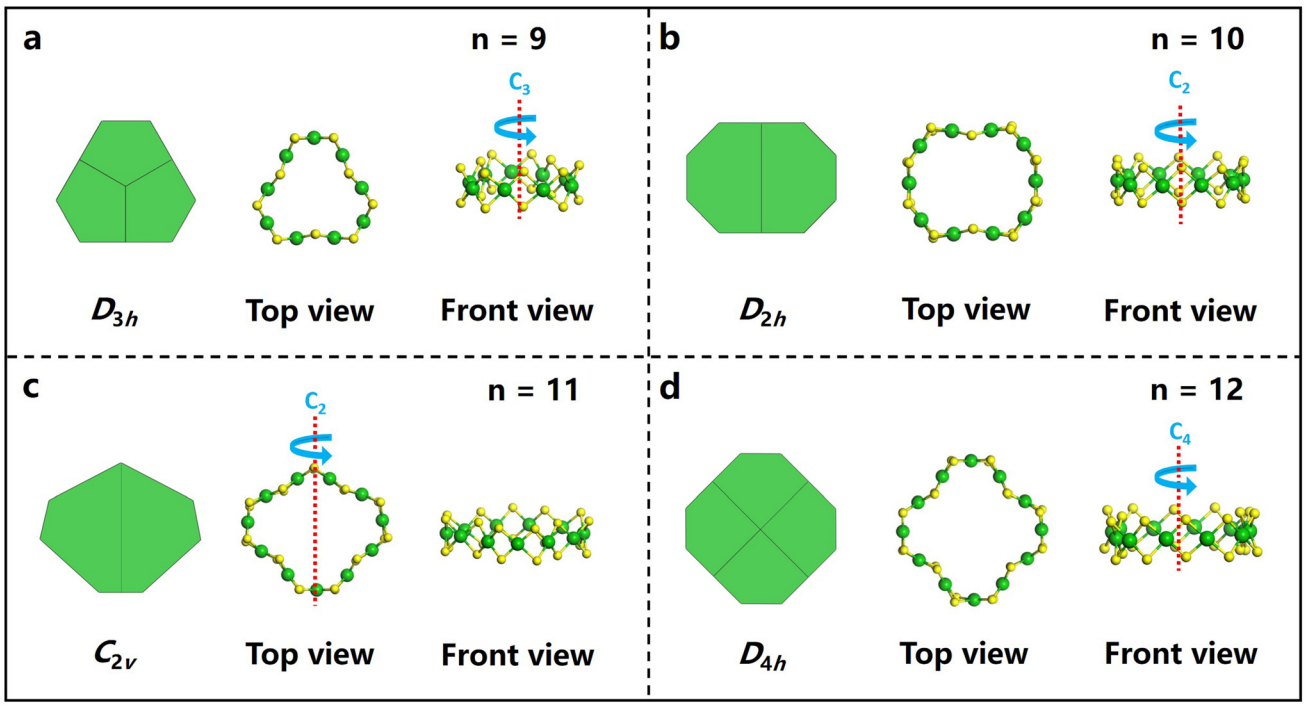

Fig. 1 Structure analysis of the $Ni_n(4MPT)_{2n}$ clusters. (a) $Ni_9(4MPT)_{18}$. (b) $Ni_{10}(4MPT)_{20}$. (c) $Ni_{11}(4MPT)_{22}$. (d) $Ni_{12}(4MPT)_{24}$. Color codes: yellow sphere, S; green sphere, Ni. All C and H atoms are omitted for clarity.

This journal is © The Royal Society of Chemistry 2024

Published on 19 January 2024. Downloaded on 7/24/2025 8:30:23 AM.

was investigated. The results indicate that these clusters show excellent catalytic activity towards the reduction of *p*-nitrophenol, and a linear correlation between catalytic activity and nickel ring size was revealed.

2. Results and discussion

The clusters were synthesized by a one-pot method. Typically, in a 50 mL round-bottomed flask, 24 mg of $NiCl_2{\cdot}6H_2O$ was dissolved in 20 mL of absolute ethanol containing 15 mg of 4MPT as the ligand, under vigorous stirring. Subsequently, 20 mg of $NaBH_4$ (which had been dissolved in 3 mL of absolute ethanol in advance) was added to the reaction solution, and the color of the solution changed from green to dark. After reacting for 12 h, the crude products were collected by centrifugation and washed with ethanol three times. 2 mL of dichloromethane (DCM) was used as the extraction agent, and the nickel cluster homologues were separated by thin layer chromatography (TLC), as shown in Fig. S1.†

To determine their precise structures, we attempted the crystallization of the as-synthesized clusters using a typical recipe involving the diffusion of methanol into a toluene-based cluster solution.[47,48] After a week, black sheets or ribbons were obtained, as shown in Fig. S1.† Single-crystal X-ray diffraction (SXRD) analysis reveals that the clusters obtained herein are members of a homologous series of macrocyclic Ni clusters, that is, $Ni_n(4MPT)_{2n}$, (n = 9–12). All the Ni clusters feature macrocyclic structures, and they may be ideally viewed as a convex n-polygon of coplanar nickel atoms with two sulfur atoms bridging each pair of adjacent nickel atoms, as shown in Fig. 1 and Fig. S2.† The Ni_nS_{2n} frameworks of $Ni_9(4MPT)_{18}$ and $Ni_{11}(4MPT)_{22}$ (Fig. 1a and c) are similar to those of $Ni_9(SPh)_{18}$ and $Ni_{11}(SPh)_{22}$;[40] however, for those of homoleptic $Ni_{10}(4MPT)_{20}$ and $Ni_{12}(4MPT)_{24}$, both frameworks are unique. The nickel–sulfur frameworks of $Ni_{10}(4MPT)_{20}$ and $Ni_{12}(4MPT)_{24}$ can be viewed as a truncated rectangle and truncated square, respectively, as shown in Fig. 1b and d, totally differing from those of $[Ni(StBu)(pyet)]_{10}$ and $[Ni(StBu)(etet)]_{12}$, in which a circular or elliptical geometry was observed.[41] Subsequently, the molecular parameters of the

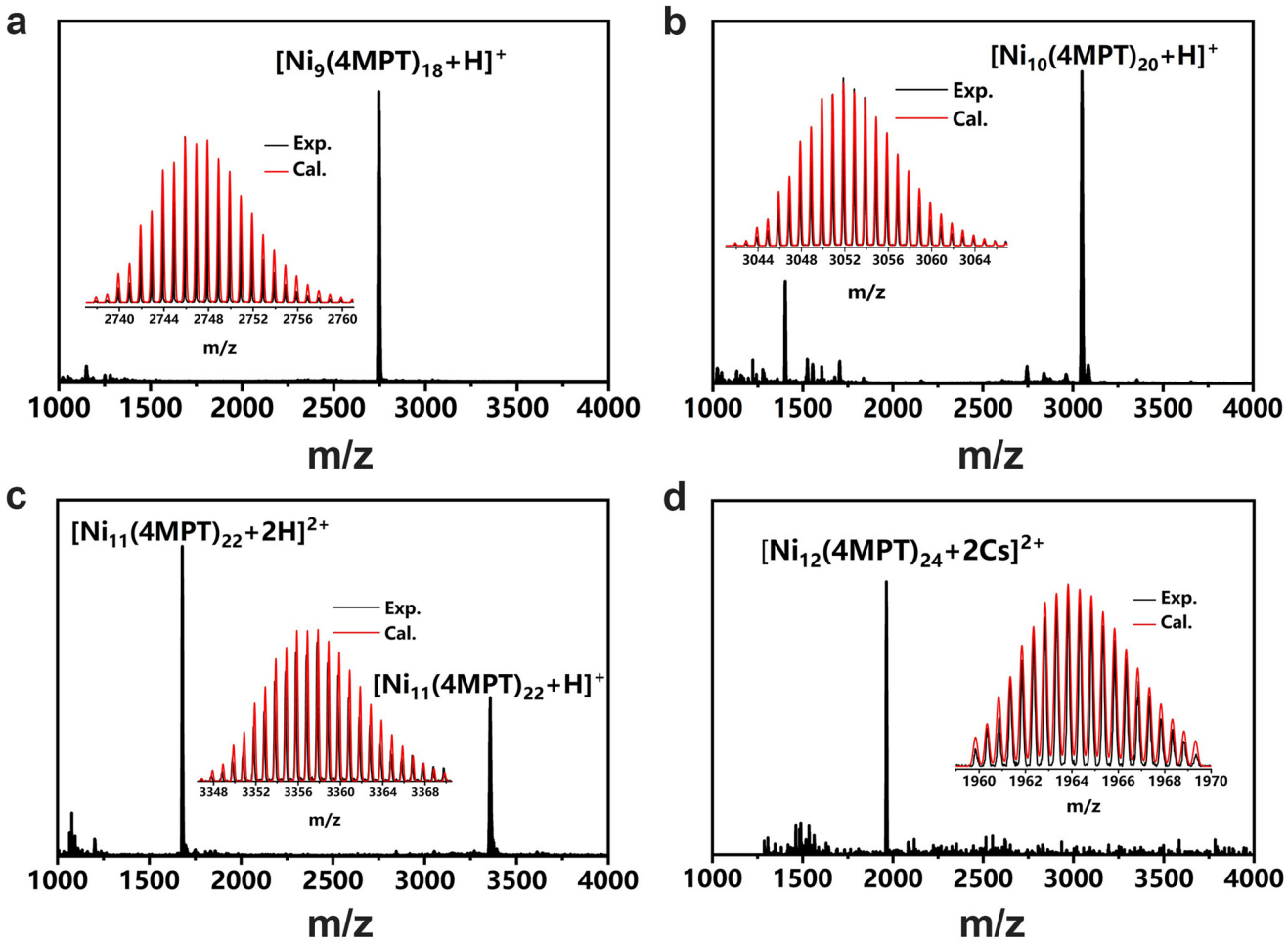

Fig. 2 ESI-MS of the $Ni_n(4MPT)_{2n}$ clusters. (a) $Ni_9(4MPT)_{18}$. (b) $Ni_{10}(4MPT)_{20}$. (c) $Ni_{11}(4MPT)_{22}$. (d) $Ni_{12}(4MPT)_{24}$. Inset: the measured (black) and simulated (red) isotopic distribution patterns of the corresponding molecular ion peaks.

Published on 19 January 2024. Downloaded on 7/24/2025 8:30:23 AM.

Ni–S framework of the $Ni_n(4MPT)_{2n}$ clusters were studied. The Ni–Ni distances, the Ni–S–Ni angles, and the Ni–S bond length of the $Ni_n(4MPT)_{2n}$ (n = 9–12) clusters are shown in Fig. S3, S4, and S5.† It is clear that the Ni_nS_{2n} frameworks of $Ni_9(4MPT)_{18}$, $Ni_{10}(4MPT)_{20}$ and $Ni_{12}(4MPT)_{24}$ are more regular than that of $Ni_{11}(4MPT)_{22}$, indicated by the more regular Ni–Ni distances, Ni–S–Ni angles, and Ni–S bond length of the $Ni_n(4MPT)_{2n}$ (n = 9, 10, 12) clusters. The top views of the Ni_nS_{2n} frameworks (n = 9, 10, 12) in Fig. 1 reveal D_{3h}, D_{2h}, and D_{4h} symmetries, respectively. Nevertheless, the $Ni_{11}S_{22}$ architecture discloses a highly deformed toroidal geometry of pseudo-C_{2v} symmetry. A detailed crystal structure analysis shows that to minimize steric interactions of the ligands, the $-PhCH_3$ substituents of the ligands in $Ni_n(4MPT)_{2n}$ (n = 9, 10, 12) were found to be sterically disposed in alternating axial and equatorial positions about the nickel rings; however, in $Ni_{11}(4MPT)_{22}$, two of the axial substituents are bent inward, resulting in distortion of the ring, as shown in Fig. S2c.† To confirm the validity of the composition and the charge state of the clusters, ESI-MS measurements were conducted, as shown in Fig. 2. The ESI-MS spectra show peaks at m/z ~2745.88, 3051.86, 3357.88, and 1963.83 Da, respectively, corresponding to the molecular ion peaks of $[Ni_9(4MPT)_{18} + H]^+$, $[Ni_{10}(4MPT)_{20} + H]^+$, $[Ni_{11}(4MPT)_{22} + H]^+$, and $[Ni_{12}(4MPT)_{24} + 2Cs]^{2+}$ adducts, as evidenced by the well-matched high-resolution experimental MS spectra compared with the calculated values of each cluster. In addition, the data were acquired in a positive model, and the results indicate that all the $Ni_n(4MPT)_{2n}$ (n = 9–12) clusters bear one or two positive charges by combining one or two H^+/Cs^+ ions. The charge states of the clusters are equal to the number of H^+ or Cs^+ ions combined, implying that these clusters are neutral.

The UV-vis-NIR spectra of the clusters are shown in Fig. 3. For each cluster, there are three featured absorption peaks located at ~345 and ~470 nm, as well as a shoulder at ~600 nm. The similar absorption profiles of the clusters imply that the electronic structures of the clusters may have something in common. Subsequently, quantum chemical calculations were carried out to reveal the electronic structures and optical behaviors of the $Ni_n(4MPT)_{2n}$ (n = 9–12) clusters. The toroidal framework of each cluster is constructed from n continuously linked planar $[NiS_4]$ subunits. The total structures of Ni clusters are distorted to D_3-$Ni_9(4MPT)_{18}$, D_2-$Ni_{10}(4MPT)_{20}$, C_1-$Ni_{11}(4MPT)_{22}$, and D_4-$Ni_{12}(4MPT)_{24}$ symmetries, respect-

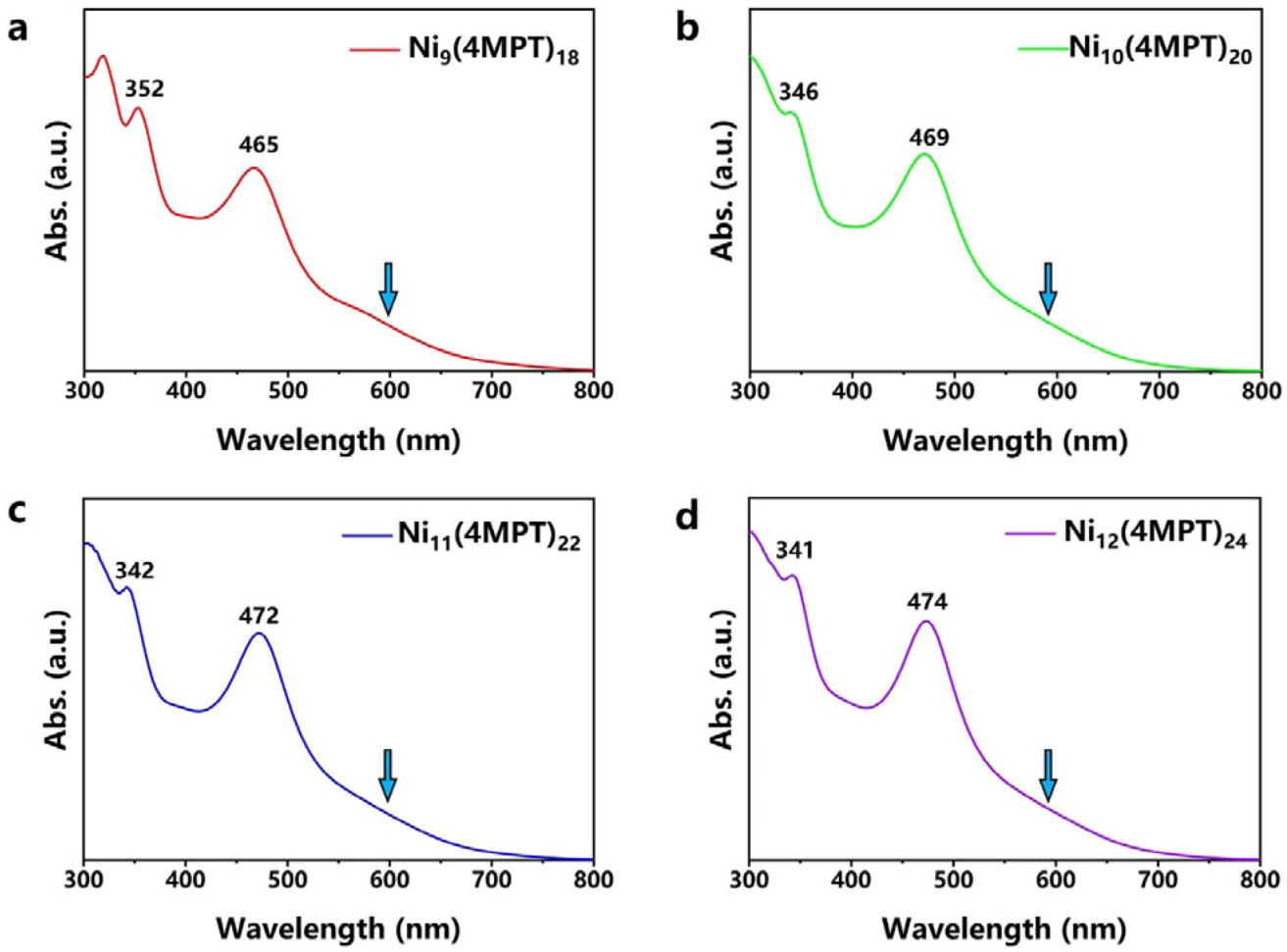

Fig. 3 UV-vis-NIR spectra of the $Ni_n(4MPT)_{2n}$ clusters. (a) $Ni_9(4MPT)_{18}$. (b) $Ni_{10}(4MPT)_{20}$. (c) $Ni_{11}(4MPT)_{22}$. (d) $Ni_{12}(4MPT)_{24}$.

 This journal is © The Royal Society of Chemistry 2024

Published on 19 January 2024. Downloaded on 7/24/2025 8:30:23 AM.

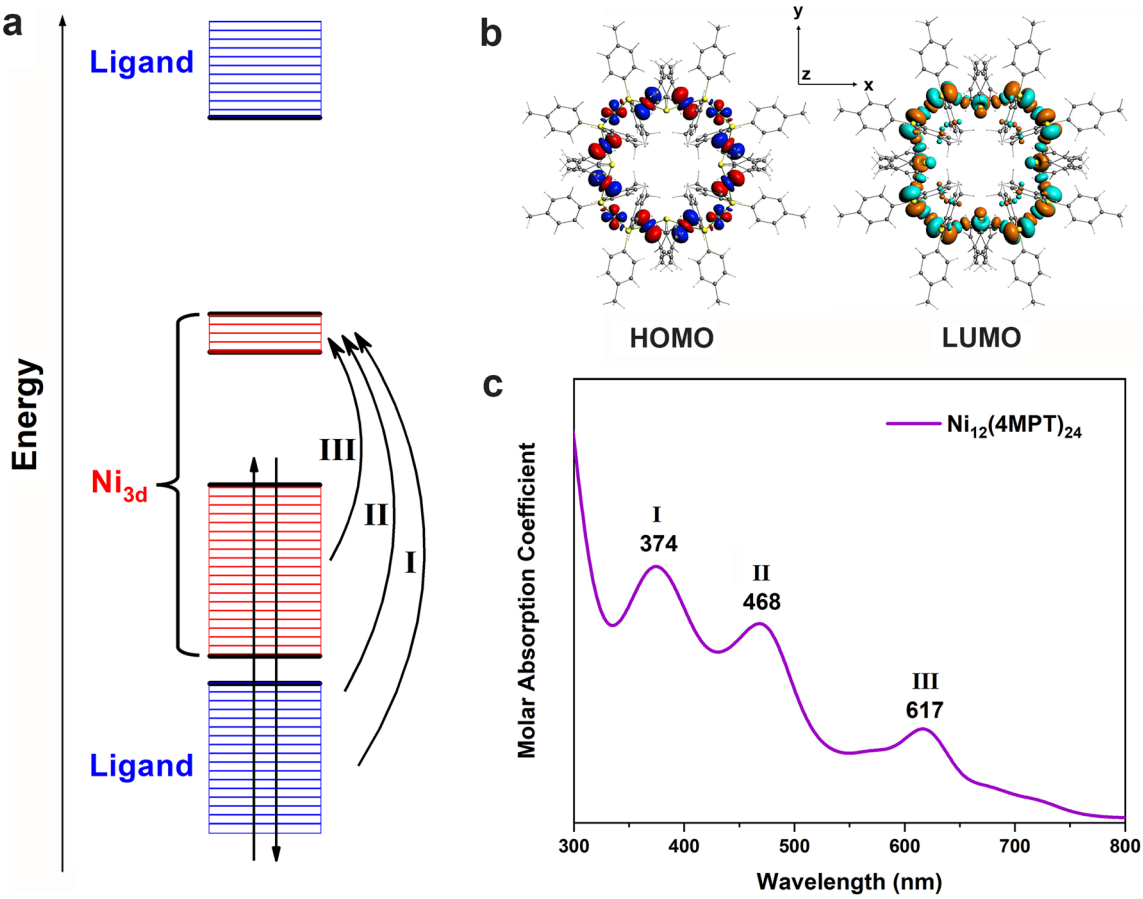

Fig. 4 Theoretical results. (a) Schematic Kohn–Sham molecular orbital energy level diagram of nickel clusters. (b) The highest occupied molecular orbital (HOMO) and lowest unoccupied molecular orbital (LUMO) of the $Ni_{12}(4MPT)_{24}$ cluster using the PBE functional (isovalue = 0.015 a.u.). (c) The simulated UV-vis spectrum of the $Ni_{12}(4MPT)_{24}$ cluster at the TDDFT/LB94 SR-ZORA level of theory with the Gaussian half-width of 45 nm, where the electron transition channels of peaks I, II, and III are shown in (a).

ively, through coordination with bridging ligands (4MPT). The Ni–Ni and Ni–S bond lengths of the optimized structures listed in Table S1† show an identical trend and agree well with those of the experimental results (see Fig. S3 and S4†). We find that the Ni clusters suggest similar electronic configurations and atomic orbital distributions, with all Ni-3d orbitals located around the Fermi level, as can be seen from the projected density of states in Fig. S6† and the schematic Kohn–Sham molecular orbital energy level diagram in Fig. 4a. Additionally, the number of vacant Ni-3d-dominated MOs is given by n and the number of occupied MOs equals $4n$, indicating the formal oxidation state of the Ni atom to be +2. There are weak bonding interactions between Ni-3d_{xy}, $d_{x^2-y^2}$, d_{z^2}, and S-2p orbitals, contributing to the nearly non-bonding HOMO and the adjacent occupied MOs, as depicted in Fig. 4b. However, the LUMO and the adjacent vacant MOs mainly arise from strong anti-bonding σ interactions between Ni-3$d_{xz,yz}$ and S-2p orbitals (see Fig. S7†), which illustrates the large HOMO–LUMO gaps and robust stabilities of Ni clusters. The computed absorption spectra and peak features from the TDDFT calculations fit well with the experimental spectra (see Fig. S8†), with the largest peak position error being 46 nm. Taking $Ni_{12}(4MPT)_{24}$ as an example, the cluster reveals three peaks (Fig. 4c), where electron excitations of strong peaks I and II correspond to transitions from the ligand-dominated orbitals in the lower and higher energy regions to vacant Ni-3d-dominated orbitals, respectively. The lower-energy peak III is weaker as it primarily comes from electron transitions between Ni-3d-dominated orbitals.

Previous studies have shown that the electronic structures of gold or silver clusters are very sensitive to their composition. In some cases, even replacing, adding or removing only one metal atom or ligand will result in an electronic structure variation of the clusters, thereby their properties.[49–51] Interestingly, for this sequence of macrocyclic nickel clusters, $Ni_n(4MPT)_{2n}$ (n = 9–12), their electronic structures did not exhibit a significant change with the increasing Ni atom number of rings, which is evidenced by similar experimental absorption spectra and the calculated HOMO–LUMO orbitals as discussed above. We believe that the similar geometries and the same Ni–S coordination of the clusters can satisfactorily explain the similarity of their electronic structures.

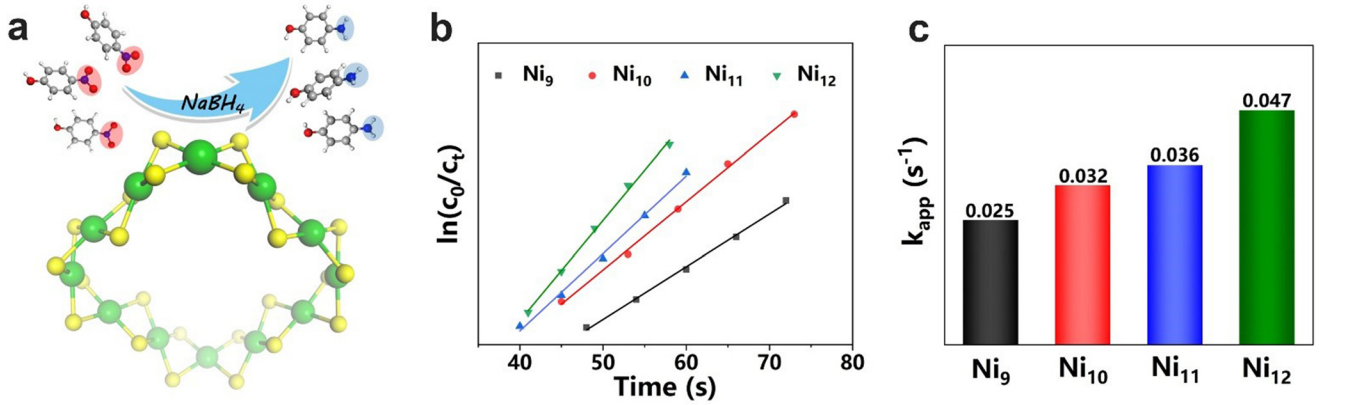

Fig. 5 Catalytic properties of the $Ni_n(4MPT)_{2n}$ (n = 9–12) clusters in the reduction reaction of *p*-nitrophenol. (a) A schematic diagram for *p*-nitrophenol reduction. (b) The corresponding reaction kinetics of the reactions. (c) Reaction rate constant (k_{app}) of the reduction reactions catalyzed by the clusters. Color codes: yellow sphere, S; green sphere, Ni. red sphere, O; blue sphere, N; gray sphere, C; white sphere, H.

Published on 19 January 2024. Downloaded on 7/24/2025 8:30:23 AM.

Due to the similarity in their geometric and electronic structures, the clusters probably exhibit similar physicochemical properties. First, the stability of the clusters was studied. As shown in Fig. S9–Fig. S12,† the clusters are very stable under diverse conditions including high temperature as well as acidic/alkaline/reductive environments, as evidenced by the negligible changes in the UV-vis spectra under each condition. Subsequently, the excellent stability of the clusters under alkaline and reductive conditions prompted us to investigate their catalytic properties in the reduction reaction of *p*-nitrophenol. As shown in Fig. 5 and Fig. S13,† the reduction of *p*-nitrophenol occurs very fast, and *p*-nitrophenol is converted into *p*-aminophenol within 2 min. Previous studies suggest that the reaction follows a quasi-first-order kinetics.[52] According to the equation, $\ln(c_0/c_t) = k_{app}t$, the slope of the line resulting from the $\ln(c_0/c_t) - t(s)$ plot gives the rate constant (k_{app}), a fundamental parameter in chemical kinetics to compare the rate of an individual reaction.[53] As shown in Fig. 5b and c, the k_{app} values for $Ni_n(4MPT)_{2n}$ (n = 9–12) are 0.025, 0.032, 0.036, and 0.047 s^{-1}, respectively. The clusters demonstrate excellent catalytic activity, and their k_{app} values exhibit an increasing trend from $Ni_9(4MPT)_{18}$ to $Ni_{12}(4MPT)_{24}$. In other words, the reaction becomes faster with increasing ring size. One possible explanation is that for the homologous series of macrocyclic Ni cluster catalysts, the number of active sites increases with the number of $[NiS_4]$ subunits in the clusters, and therefore a faster reaction results.

3. Conclusions

In summary, we, for the first time, have reported a series of macrocyclic homoleptic nickel clusters $Ni_n(4MPT)_{2n}$ (n = 9–12), and their compositions and structures were determined by using SXRD and ESI-MS. Although the clusters possess ring-like structures, the $Ni_{10}(4MPT)_{20}$ and $Ni_{12}(4MPT)_{24}$ clusters are unique and distinct from those of their reported Ni_{10} and Ni_{12} counterparts. More interestingly, the electronic structures and optical properties do not show significant changes with the increase of the Ni atoms. Finally, the reduction of *p*-nitrophenol catalyzed by these clusters was studied, and the clusters display excellent catalytic activity towards the reduction of *p*-nitrophenol. The rate constant exhibits an increasing trend from $Ni_9(4MPT)_{18}$ to $Ni_{12}(4MPT)_{24}$, which implies that the catalytic activity is positively correlated with the size of the Ni–S ring. The study provides a facile approach to macrocyclic homoleptic nickel clusters, and we anticipate that the work reported herein will benefit the fabrication of other metal macrocyclic homoleptic clusters consisting of group 10 transition elements, and contributes to an in-depth understanding of their structure–property correlations at the atomic level.

Author contributions

C. Y. conceived and designed the experiments. C. X. and J. L. performed quantum chemical calculations and analyzed the data. H. X. and R. C. synthesized the samples and performed the measurements. C. R., C. M., Y. G., and W. C. analyzed parts of the data and plotted the figures. Y. Z. collected and refined the crystal data of the clusters. C. Y., H. X., and C. X. wrote the paper.

Conflicts of interest

There are no conflicts to declare.

Acknowledgements

This work was financially supported by start-up research funding of Fujian Normal University, the Natural Science Foundation of Ningbo (202003N4005), the National Natural Science Foundation of China (No. 22033005 and 22103035) and National Key Research and Development Project

This journal is © The Royal Society of Chemistry 2024

Published on 19 January 2024. Downloaded on 7/24/2025 8:30:23 AM.

(2022YFA1503900). Computational resources were provided by the CHEM high-performance supercomputer cluster (CHEM-HPC) and Center for Computational Science and Engineering at Southern University of Science and Technology.

References

1 X. Zou, X. Kang and M. Zhu, *Chem. Soc. Rev.*, 2023, **52**, 5892–5967.
2 Y. Jin, C. Zhang, X.-Y. Dong, S.-Q. Zang and T. C. W. Mak, *Chem. Soc. Rev.*, 2021, **50**, 2297–2319.
3 Z. J. Guan, J. J. Li, F. Hu and Q. M. Wang, *Angew. Chem., Int. Ed.*, 2022, **61**, e202209725.
4 X. J. Wang, B. Yin, L. R. Jiang, C. Yang, Y. Liu, G. Zou, S. Chen and M. Z. Zhu, *Science*, 2023, **381**, 784–790.
5 Y. Li, Y. Song, X. Zhang, T. Liu, T. Xu, H. Wang, D.-e. Jiang and R. Jin, *J. Am. Chem. Soc.*, 2022, **144**, 12381–12389.
6 L. Tang, B. Wang, R. Wang and S. Wang, *Nanoscale*, 2023, **15**, 1602–1608.
7 T. Jia, Z.-J. Guan, C. Zhang, X.-Z. Zhu, Y.-X. Chen, Q. Zhang, Y. Yang and D. Sun, *J. Am. Chem. Soc.*, 2023, **145**, 10355–10363.
8 Z.-M. Zhu, Y. Zhao, H. Zhao, C. Liu, Y. Zhang, W. Fei, H. Bi and M.-B. Li, *Nano Lett.*, 2023, **23**, 7508–7515.
9 Z. Zuo, K.-J. Hu, S. Lu, S. Hu, S. Tang, Y. Zhang, Z. Zhao, D. Zheng and F. Song, *Nanoscale*, 2023, **15**, 15043–15049.
10 P. D. Jadzinsky, G. Calero, C. J. Ackerson, D. A. Bushnell and R. D. Kornberg, *Science*, 2007, **318**, 430–433.
11 F. Hu, R. L. He, Z. J. Guan, C. Y. Liu and Q. M. Wang, *Angew. Chem., Int. Ed.*, 2023, **62**, e202304134.
12 Y. Cao, Y. Xu, H. Shen, P. Pan, X. Zou, X. Kang and M. Zhu, *Nanoscale*, 2023, **15**, 13784–13789.
13 L. Fang, W. Fan, G. Bian, R. Wang, Q. You, W. Gu, N. Xia, L. Liao, J. Li, H. Deng, N. Yan and Z. Wu, *Angew. Chem., Int. Ed.*, 2023, **62**, e202305604.
14 J. Tang, C. Liu, C. Zhu, K. Sun, H. Wang, W. Yin, C. Xu, Y. Li, W. Wang, L. Wang, R. Wu, C. Liu and J. Huang, *Nanoscale*, 2023, **15**, 2843–2848.
15 C. Xu, Y. Jin, H. Fang, H. Zheng, J. C. Carozza, Y. Pan, P.-J. Wei, Z. Zhang, Z. Wei, Z. Zhou and H. Han, *J. Am. Chem. Soc.*, 2023, **145**, 25673–25685.
16 L. Li, P. Wang and Y. Pei, *Nanoscale*, 2022, **14**, 5694–5700.
17 G. Yang, X. Pan, W. Feng, Q. Yao, F. Jiang, F. Du, X. Zhou, J. Xie and X. Yuan, *ACS Nano*, 2023, **17**, 15605–15614.
18 P. Woodward, L. F. Dahl, E. W. Abel and B. C. Crosse, *J. Am. Chem. Soc.*, 1965, **87**, 5251–5253.
19 E. W. Abel and B. C. Crosse, *J. Chem. Soc. A*, 1966, 1377–1378.
20 R. Angamuthu, H. Kooijman, M. Lutz, A. L. Spek and E. Bouwman, *Dalton Trans.*, 2007, 4641–4643.
21 M. Zhu, S. Zhou, C. Yao, L. Liao and Z. Wu, *Nanoscale*, 2014, **6**, 14195–14199.
22 C. Tan, M. Jin, H. Zhang, S. Hu, T. Sheng and X. Wu, *CrystEngComm*, 2015, **17**, 5110–5115.
23 D. R. Kauffman, D. Alfonso, D. N. Tafen, J. Lekse, C. Wang, X. Deng, J. Lee, H. Jang, J.-s. Lee, S. Kumar and C. Matranga, *ACS Catal.*, 2016, **6**, 1225–1234.
24 X. Chai, T. Li, M. Chen, R. Jin, W. Ding and Y. Zhu, *Nanoscale*, 2018, **10**, 19375–19382.
25 M. P. Maman, T. Gurusamy, A. K. Pal, R. Jana, K. Ramanujam, A. Datta and S. Mandal, *Angew. Chem., Int. Ed.*, 2023, **62**, e202305462.
26 H. Seong, J. Kim, K. Chang, H.-w. Kim, W. Choi and D. Lee, *J. Electrochem. Sci. Technol.*, 2023, **14**, 243–251.
27 A. Datta, N. S. John, G. U. Kulkarni and S. K. Pati, *J. Phys. Chem. A*, 2005, **109**, 11647–11649.
28 H. N. Kagalwala, E. Gottlieb, G. Li, T. Li, R. Jin and S. Bernhard, *Inorg. Chem.*, 2013, **52**, 9094–9101.
29 K. S. Joya, L. Sinatra, L. G. AbdulHalim, C. P. Joshi, M. N. Hedhili, O. M. Bakr and I. Hussain, *Nanoscale*, 2016, **8**, 9695–9703.
30 S. Srinivasan, Z. Liu, S. House and R. Jin, *Inorg. Chem.*, 2022, **62**, 1875–1884.
31 S. Funaki, T. Kawawaki, T. Okada, K. Takemae, S. Hossain, Y. Niihori, T. Naito, M. Takagi, T. Shimazaki, S. Kikkawa, S. Yamazoe, M. Tachikawa and Y. Negishi, *Nanoscale*, 2023, **15**, 5201–5208.
32 A. J. Touchton, G. Wu and T. W. Hayton, *Small*, 2021, **17**, 2003133.
33 A. H. Mahmoudkhani and V. Langer, *Polyhedron*, 1999, **18**, 3407–3410.
34 C. Tan, M. Jin, X. Ma, Q. Zhu, Y. Huang, Y. Wang, S. Hu, T. Sheng and X. Wu, *Dalton Trans.*, 2012, **41**, 8472–8476.
35 T. Krüger, B. Krebs and G. Henkel, *Angew. Chem., Int. Ed.*, 2003, **28**, 61–62.
36 Q. You, X.-L. Jiang, W. Fan, Y.-S. Cui, Y. Zhao, S. Zhuang, W. Gu, L. Liao, C.-Q. Xu, J. Li and Z. Wu, *Angew. Chem., Int. Ed.*, 2023, e202313491.
37 S. Havenridge and C. M. Aikens, *J. Phys. Chem. A*, 2023, **127**, 9932–9943.
38 I. G. Dance, M. L. Scudder and R. Secomb, *Inorg. Chem.*, 1985, **24**, 1201–1208.
39 T. Kruger, B. Krebs and G. Henkel, *Angew. Chem., Int. Ed. Engl.*, 1989, **28**, 61–62.
40 S. A. Ivanov, M. A. Kozee, W. A. Merrill, S. Agarwal and L. F. Dahl, *J. Chem. Soc., Dalton Trans.*, 2002, 4105–4115.
41 C. Zhang, T. Matsumoto, M. Samoc, S. Petrie, S. Meng, T. C. Corkery, R. Stranger, J. Zhang, M. G. Humphrey and K. Tatsumi, *Angew. Chem., Int. Ed.*, 2010, **49**, 4209–4212.
42 O. L. Sydora, P. T. Wolczanski, E. B. Lobkovsky, E. Rumberger and D. N. Hendrickson, *Chem. Commun.*, 2004, 650–651.
43 H. Xiang, H. Yan, J. Liu, R. Cheng, C. Q. Xu, J. Li and C. Yao, *J. Am. Chem. Soc.*, 2022, **144**, 14248–14257.
44 C. Yao, C. Q. Xu, I. H. Park, M. Zhao, Z. Zhu, J. Li, X. Hai, H. Fang, Y. Zhang, G. Macam, J. Teng, L. Li, Q. H. Xu, F. C. Chuang, J. Lu, C. Su, J. Li and J. Lu, *Angew. Chem., Int. Ed.*, 2020, **59**, 8270–8276.
45 C. J. Zeng, C. Y. Liu, Y. Pei and R. C. Jin, *ACS Nano*, 2013, **7**, 6138–6145.

46 H. Yan, H. Xiang, J. Liu, R. Cheng, Y. Ye, Y. Han and C. Yao, *Small*, 2022, **18**, e2200812.
47 C. Yao, N. Guo, S. Xi, C.-Q. Xu, W. Liu, X. Zhao, J. Li, H. Fang, J. Su, Z. Chen, H. Yan, Z. Qiu, P. Lyu, C. Chen, H. Xu, X. Peng, X. Li, B. Liu, C. Su, S. J. Pennycook, C.-J. Sun, J. Li, C. Zhang, Y. Du and J. Lu, *Nat. Commun.*, 2020, **11**, 4389.
48 C. Ruan, H. Xiang, H. Yan, Y. Deng, Y. Zhao, C. Q. Xu, J. Li and C. Yao, *Small*, 2023, **19**, 2305056.
49 C. Dong, R. W. Huang, A. Sagadevan, P. Yuan, L. Gutiérrez-Arzaluz, A. Ghosh, S. Nematulloev, B. Alamer, O. F. Mohammed, I. Hussain, M. Rueping and O. M. Bakr, *Angew. Chem., Int. Ed.*, 2023, **62**, e202307140.
50 Y. Li, H. K. Kim, R. D. McGillicuddy, S.-L. Zheng, K. J. Anderton, G. J. Stec, J. Lee, D. Cui and J. A. Mason, *J. Am. Chem. Soc.*, 2023, **145**, 9304–9312.
51 C. Yao, Y.-j. Lin, J. Yuan, L. Liao, M. Zhu, L.-h. Weng, J. Yang and Z. Wu, *J. Am. Chem. Soc.*, 2015, **137**, 15350–15353.
52 Z. J. Guan, R. L. He, S. F. Yuan, J. J. Li, F. Hu, C. Y. Liu and Q. M. Wang, *Angew. Chem., Int. Ed.*, 2022, **61**, e202116965.
53 S. Song, Y. Wang, H. Shen, J. Zhang, H. Mo, J. Xie, N. Zhou and J. Shen, *ACS Appl. Nano Mater.*, 2019, **2**, 7074–7084.

Published on 19 January 2024. Downloaded on 7/24/2025 8:30:23 AM.

This journal is © The Royal Society of Chemistry 2024